Investigating OVI Emission Towards the Loop I Superbubble[1]

Hiroki Yamashita

Faculty Sponsor: Shauna Sallmen, Department of Physics

ABSTRACT

The material between stars (interstellar medium) shows bubble-like features, expanding at several hundreds km/s and filled with hot gas. Diffuse hot gas is expected to produce O VI emission. The Local Bubble, surrounding the Sun, was once believed to be filled with hot gas, but recent observations have made the situation unclear. The Loop I superbubble, believed to be blown by strong stellar winds or supernovae, appears to be interacting with the Local Bubble. In this experiment, a comparison is made between Far Ultraviolet Spectroscopic Explorer (*FUSE*) satellite observations of two adjacent pointing directions towards the Interaction Zone between the two bubbles. In one direction (Shadowed sightline), cold gas in the Interaction Zone blocks the distant O VI emission but such distant emission is not blocked in the other direction (Unshadowed sightline). Comparing intensities of O VI emission from these two sightlines allows us to specify the location of O VI-emitting gas. The data show that O VI emission from the Shadowed sightline is much less than from the Unshadowed sightline. This indicates that there is little or no O VI-emitting gas inside our Local Bubble, and the O VI-emitting gas is located inside or beyond the Loop I superbubble.

INTRODUCTION

Our sun and the solar system are located inside the Milky Way Galaxy, which consists of a disk of stars, plus a spherical bulge and halo of older stars. The galaxy contains about 100 billion stars and is about 9.25×10^{17} km across. The sun is about 8000 pc from the center of the Milky Way's disk (1 pc = 3.26 light years = 3.1×10^{13} km). In addition to planets and stars, our galaxy contains material called the interstellar medium (ISM). This gas and dust between stars is located mainly in the galactic disk and has temperatures between –253°C and 20 million °C.

In recent years, several detections of galactic O VI (O^{+5}) emission have been made with the *FUSE* (Far Ultraviolet Spectroscopic Explorer) satellite. Typical values at 1032 Å (1Å = 0.1 nm) in directions with small amounts of neutral hydrogen are 2000-3300 photons cm^{-2} s^{-1} sr^{-1} (LU) (Dixon et al. 2001; Shelton et al. 2001; Shelton 2002, 2003; Welsh et al. 2002). Until recently, the galactic location of this hot-gas emission was unknown. Shelton (2003) concludes that the local (< 230 pc) contribution to this emission is negligible, with a 2σ upper limit of 500 photons cm^{-2} s^{-1} sr^{-1} in the direction galactic coordinates (l,b) = (278.6º, -45.3º). It therefore appears that most of this emission arises from hot gas in the Galactic Halo.

Gas in the galactic interstellar medium is heated by energy input from stellar winds and supernova (exploding star) events. These processes are responsible for redistributing energy and material throughout our galaxy, resulting in the formation of new generations of stars. The non-uniform interstellar gas exhibits a complex set of interacting shells, bubble-like structures, "chimneys", and worms that are seen as evidence of stellar energy input. Although the physical state and evolution of these gas phases have been broadly explained, it has not yet been determined whether the ISM is best described by a three-phase model (McKee & Ostriker 1977), a galactic fountain model (Shapiro & Field 1976), or a model with more isolated supernova remnants (Cox & Smith 1974; Slavin & Cox 1993). There are still many outstanding problems with these (and all other current) models of the ISM.

Superbubbles are extremely large structures in the ISM, believed to be blown by the combined energy output of a cluster of stars. Such regions provide an important diagnostic of the processes by which supernovae and stellar winds control the overall evolution of our galaxy. Superbubbles are expected to be filled with hot emitting gas. The O VI ion, characteristic of gas with a temperature of 300,000 K, is a sensitive probe of this material. In this paper, a shadowing strategy is used to determine the location of hot emitting gas towards the Loop I superbubble.

[1] Based on observations made with the NASA-CNES-CSA Far Ultraviolet Spectroscopic Explorer. FUSE is operated for NASA by the Johns Hopkins University under NASA contract NAS5-32985.

Observations for the adjacent sightlines were made to compare the intensity of emission from each sightline. Since one sight line blocks the distant emission and the other does not, intensities from each sight line are different. This difference in intensity tells us the location of hot emitting gas.

DESCRIPTION OF THE REGION

Loop I is a large-scale structure first discovered in the radio continuum sky (Berkhuijsen et al. 1971). The 116º ± 4º radio ring is centered on galactic coordinates (*l*,*b*) = (329º ± 1.5º, 17.5º ± 3º). It is widely believed to be a superbubble blown by strong stellar winds and supernovae of the Sco-Cen OB association (~170 pc away). X-ray, neutral-hydrogen, and optical absorption measurements are consistent with a shell of radius ~100 pc centered ~130 pc away in the direction (*l*,*b*) = (330º, 15º), with the receding shell < 212 pc away (Nishikida 1999).

Egger & Aschenbach (1995) identified an annular structure seen inside the Loop I H I shell in the H I map of Dickey and Lockman (1990). This feature is interpreted as the interaction zone between Loop I and our Local Bubble. Using data compiled by Fruscione et al. (1994), Egger & Aschenbach determined that its distance is ~70 pc and the neutral hydrogen column density N_H jumps from less than 10^{20} cm^{-2} to over 7 x 10^{20} cm^{-2} at this distance.

Figure 1 shows the neutral hydrogen image of this region of the sky, taken from Dickey & Lockman (1990). The Interaction Zone (IZ) is outlined for ease of identification. Our region of interest lies inside the small trapezoidal region indicated on the Figure. The 1/4 keV X-ray map for this small region is shown in Figure 2 (Snowden et al. 1997). The "Shadowed" sightline intersects the neutral-hydrogen interaction zone, while the "Unshadowed" sightline passes through an adjacent region of low neutral-hydrogen column density. The neutral gas blocks high-energy photons, causing the X-ray shadowing effect seen in the ROSAT image. This same material will block distant O VI emission. Comparison of the two sightlines gives us the opportunity to distinguish between local and distant emission.

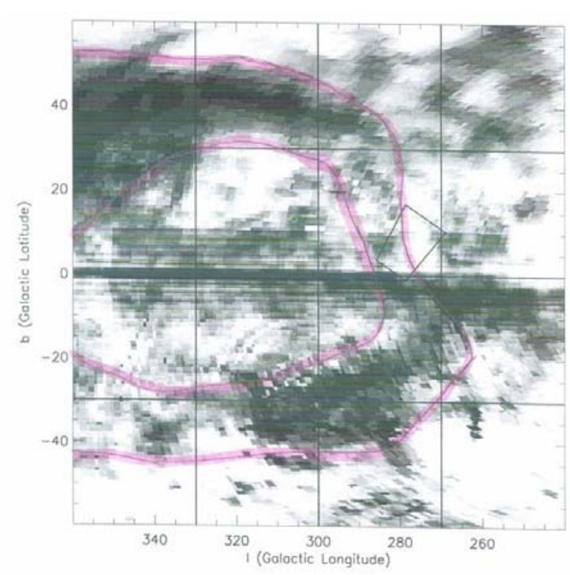

Figure 1. Neutral Hydrogen map (Dickey & Lockman 1990) showing the Interaction Zone. Darker areas contain more neutral hydrogen. The region shown in Figure 2 is indicated by the trapezoid.

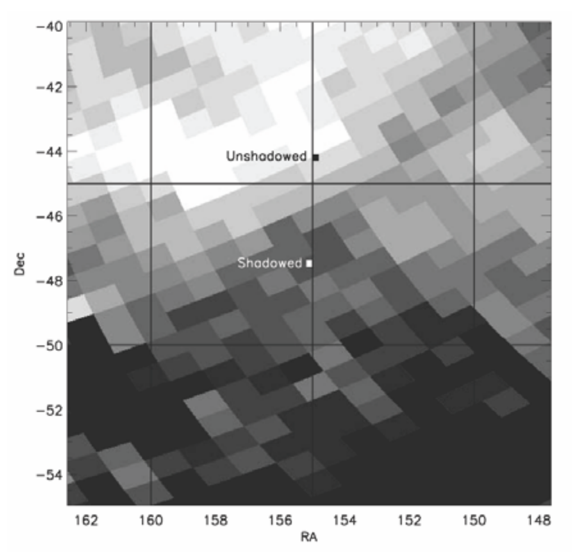

Figure 2. 1/4 keV ROSAT map showing our sightlines (Snowden et al. 1997). More X-rays are received from brighter areas. Note the X-ray shadowing due to the neutral hydrogen in the IZ.

Figure 3 schematically shows the Local bubble, Loop I superbubble, and the Interaction zone between them. The lines of sight are shown for each direction of observation.

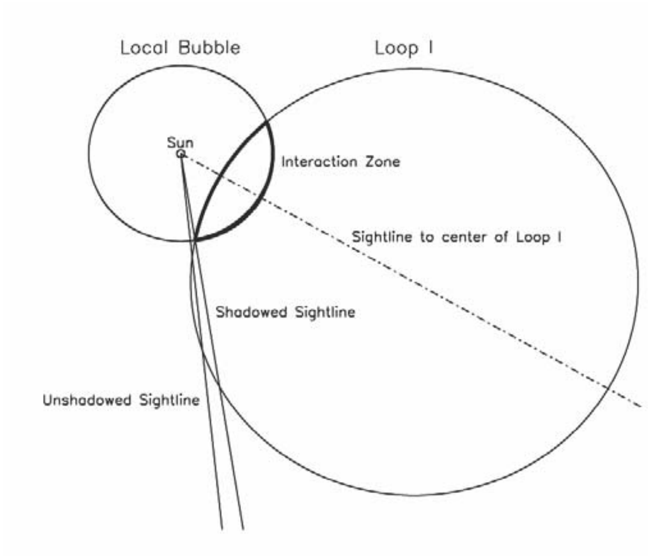

Figure 3. Schematic Diagram showing the relative locations of the Sun, Local Bubble, Loop I superbubble, Interaction Zone, and our sightlines.

OBSERVATIONS

FUSE consists of four separate optical systems. Two employ LiF optical coatings and are sensitive to wavelengths from 990 to 1187 Å, while the other two use SiC coatings, which provide reflectivity to wavelengths as short as 905 Å. The four channels overlap in the astrophysically important 990-1070 Å region. For a complete description of *FUSE*, its mission, and its in-flight performance, see Moos et al. (2000) and Sahnow et al. (2000).

The *FUSE* spectrum of the "Shadowed" sightline was obtained in 3 observations (C1640401, C1640402, and C1640403). The first two were obtained on 2002 June 27-29, and the third on 2003 February 18/19. Each exposure was centered on (*l*,*b*) = (278.23º, +8.02º). The total usable exposure time for LiF 1a was 60,460 sec, with 40,635 sec obtained in orbital night. Data for the "Unshadowed" sightline (C1640301), centered on (*l*,*b*) = (276.26º, +10.692º), were obtained on 2004 April 3/4. The total usable LiF 1a exposure time was 42,600 sec, with 29,910 obtained during orbital night.

Data were reduced using CalFUSE v3.0.7. The data reduction process includes burst screening, removal of data obtained during passages through the South Atlantic Anomaly or at low earth-limb angles, pulse height screening, corrections for spacecraft motions, and dead-time correction. The pipeline also performs an initial wavelength calibration as well as flux calibration, with an estimated uncertainty of ~10% (Sahnow et al 2000). Background removal was suppressed.

To reduce the background noise contribution, non-standard pulse height screening parameters were used. Chosen pulse heights were 8-28 for Shadowed (C16404) and 6-31 for Unshadowed (C16403). Tests were performed to ensure that these values did not remove real photons while reducing the background noise.

The exposures for each observation were added together prior to final spectral extraction. In addition, all data were processed once including photons from both orbital day and orbital night, and once including only those from orbital night. Wavelength calibration was done by measuring the observed heliocentric wavelengths of airglow lines for each observation, and applying the measured offset (no other term was deemed necessary) to the spectrum (converting the expected airglow wavelengths to heliocentric for each observation). After this, multiple observations were combined on the corrected heliocentric scale, if necessary. Systematic errors in wavelength are estimated to be 15 km s^{-1} or 0.052 Å.

RESULTS

The resulting spectra for the two sightlines are shown in Figures 4 and 5. Only nighttime spectra are shown, as several others have noted an apparent airglow feature near 1032 Å (Welsh et al. 2002; Shelton 2002). No such feature is detectable in our data, and the nighttime measurements, although of lower SNR, are entirely consistent with the spectra produced by including daytime data. Various airglow lines are visible, as are the two emission lines of the O VI doublet. The 1038Å line is blended with a 1037Å C II* emission line. The intensities of these lines were measured as follows.

Each emission line was assumed to be described by 106 km s^{-1} tophat (instrumental response to a filled aperture) convolved with a Gaussian. This appears to be correct for LiF 1a, but the airglow lines appear somewhat narrower for other detector segments. The lines were fit using the IDL-based MPFIT routines developed by Craig Markwardt[2]. Initially, only the 1032 Å line was included in the fit (top panel). Since the C II* emission line at 1037 Å is mixed with the O VI emission line at 1038 Å, we assume that the 1038 Å O VI emission line is half the intensity of the O VI emission line at 1032 Å. This assumption is true for optically thin gas, and yields reasonable results in this case. This O VI fitted model was removed from the entire spectrum, leaving the C II* emission line (middle panel). The C II* emission line was then fitted in the same way as the O VI emission line. The reasonableness of the resulting C II* fits validates this procedure. The complete model is shown over the original spectrum in the bottom panel.

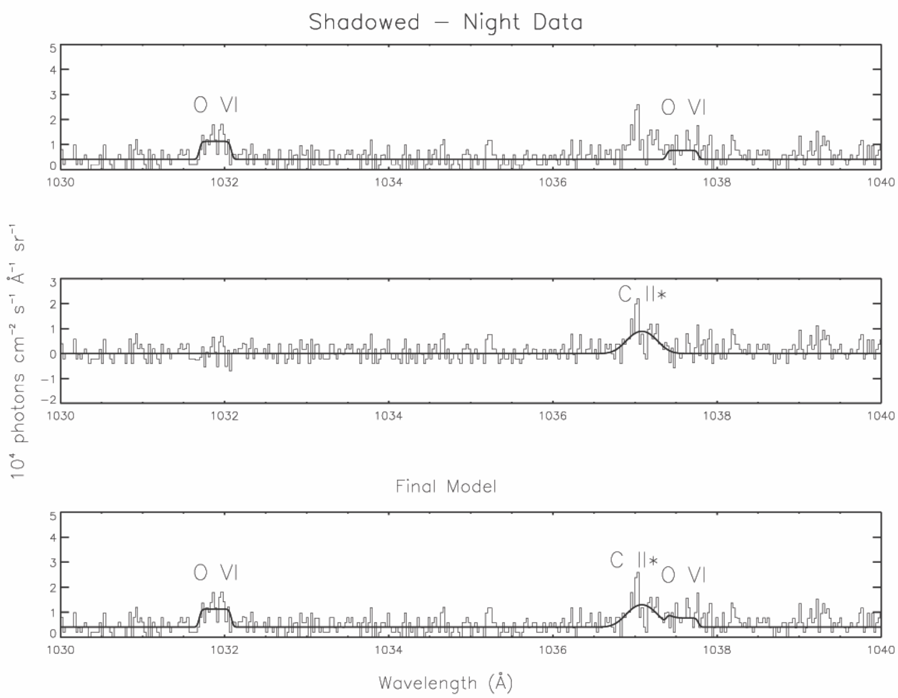

Figure 4. Spectrum for Shadowed sightline: Top: fit to OVI; Middle: fit to C II*; Bottom: full fit.

[2] http://cow.physics.wisc.edu/~craigm/idl/idl.html

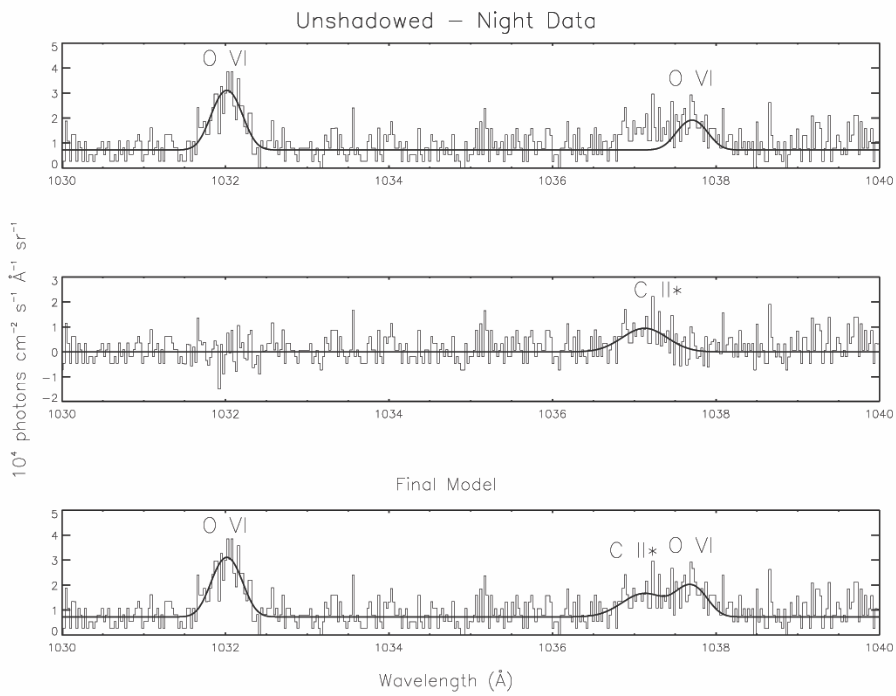

Figure 5. Spectrum for Unshadowed sightline, as in Figure 4

The results of the fits are reported in Table 1. The heliocentric wavelengths yield a heliocentric radial velocity and have been converted to the standard Local Standard of Rest (LSR) in the table. The results for C II* have not been included here, as they will be discussed in a separate paper (Sallmen, Korpela, & Yamashita, in preparation).

Table 1. O VI Emission Measurements

Sightline	Data	l (º)	b (º)	O VI Intensity (LU)	Width (Å)	V_{LSR} (km s^{-1})
Shadowed	Night	278.23	+8.02	2800 ± 500	.02 ± .03	–26 ± 4
Shadowed	Day + Night	278.23	+8.02	3200 ± 500	.10 ± .05	–28 ± 7
Unshadowed	Night	276.26	+10.69	10800 ± 1150	.13 ± .03	11 ± 6
Unshadowed	Day + Night	276.26	+10.69	9400 ± 950	.12 ± .02	10 ± 6

ANALYSIS

The observed intensities for the shadowed and unshadowed sightlines are $I_{shadowed} = 2800 \pm 500$ photons cm^{-2} s^{-1} sr^{-1} and $I_{unshadowed} = 10800 \pm 1150$ photons cm^{-2} s^{-1} sr^{-1}. To interpret our data, we made several assumptions and used the following two equations for the intensity of emission from each sightline:

$$I_{shadowed} = I_{LB} + I_{beyond} \times e^{-\tau}$$
$$I_{unshadowed} = I_{LB} + I_{beyond}$$

where I_{LB} indicates the intensity of emission from Local Bubble, and I_{beyond} indicates the intensity of emission from beyond the shadowing material, which has optical depth τ. In one case, we assumed that the shadowing material in the Interaction Zone was completely opaque ($\tau = \infty$). In this case, $I_{LB} = 2800 \pm 500$ photons cm^{-2} s^{-1} sr^{-1} and $I_{beyond} = 8000 \pm 1150$ photons cm^{-2} s^{-1} sr^{-1}. In the second case, we assumed that no emission arose within the Local Bubble ($I_{LB} = 0$), reflecting the recent results of Shelton (2003). This yields $I_{beyond} = 10800 \pm 1150$ photons cm^{-2} s^{-1} sr^{-1}, optical depth $\tau = 1.35 \pm 0.3$, and the column density of neutral hydrogen in the Interaction Zone $N(H\ I)_{IZ} = 4 \pm 0.3 \times 10^{20}$ cm^{-2} (assuming $N(H\ I) = 3 \times 10^{20}$ cm^{-2} for $\tau = 1$). Finally, we assumed that the shadowing material in this region had the average properties of the Interaction zone. Under these assumptions $N(H\ I)_{IZ} = 7 \times 10^{20}$ cm^{-2}, $\tau = 2.3$, $I_{LB} = 1900 \pm 600$ photons cm^{-2} s^{-1} sr^{-1}, and $I_{bey} = 8900 \pm 1400$ photons cm^{-2} s^{-1} sr^{-1}. The results of these calculations are summarized in Table 2.

Table 2. Analysis of Results

Assumptions	I_{LB} (photons cm^{-2} s^{-1} sr^{-1})	I_{beyond} (photons cm^{-2} s^{-1} sr^{-1})	τ_{IZ}	$N(HI)_{IZ}$ (cm^{-2}) (calculated from τ_{IZ})
IZ completely opaque ($\tau_{IZ} = \infty$)	2800 ± 500	8000 ± 1150	∞	∞
No emission from the LB ($I_{LB} = 0$)	0	10800 ± 1150	1.35 ± 0.3	$4 \pm 0.3 \times 10^{20}$
Average properties of the IZ ($\tau_{IZ} = 2.3$)	1900 ± 600	8900 ± 1400	2.3	7×10^{20}

We also used the Dickey & Lockman (1990) measurements of total (to infinite distance) column density of neutral hydrogen for both sightlines, and assumed that the difference between them was due to neutral hydrogen in the Interaction Zone. This allowed us to estimate τ for the IZ. With $N(H\ I)_{unsh} = 1.26 \times 10^{21}$ cm^{-2} and $N(H\ I)_{shad} = 1.41 \times 10^{21}$ cm^{-2}, $N(H\ I)_{IZ} = N(H\ I)_{shad} - N(H\ I)_{unsh} = 1.51 \times 10^{20}$ cm^{-2}, giving $\tau = 0.503$. This assumption yielded $I_{beyond} = 20300$ photons cm^{-2} s^{-1} sr^{-1} and $I_{LB} = -9500$ photons cm^{-2} s^{-1} sr^{-1}. The negative intensity for I_{LB} is not acceptable. Therefore, this assumption is not correct, and neutral hydrogen differences in the two directions are not due only to the Interaction Zone.

In all cases, the local contribution to the emission is small, indicating that most of the emission lies beyond our Local Bubble. The estimated intensity of the more distant emission is significantly larger than the typical measurement (~2500 photons cm^{-2} s^{-1} sr^{-1}) for directions of low hydrogen column density. Given the total $N(H\ I) \sim 10^{21}$ cm^{-2} along our sightlines, O VI emission from the galactic halo would be attenuated by a factor of ~ 20 ($e^{-3} \sim 0.05$). Under any reasonable assumptions, a significant portion of our detected emission must be associated with the Loop I Superbubble itself. Further study will be required to determine how much of this emission arises from hot gas filling the bubble, and how much from hot gas mixing with cooler gas at the interfaces within the Interaction Zone.

CONCLUSIONS

We used *FUSE* to observe OVI emission from two sightlines next to each other in order to specify the location of hot emitting gas towards the Loop I Superbubble. Using a shadowing strategy, two sightlines centered on (l,b) = (278.23º, +8.02º) and (l,b) = (276.26º, +10.692º) were observed. The measured OVI emission intensities from these two sightlines were compared. Because cold neutral hydrogen gas in the Interaction Zone blocks the distant emission from one direction but not from the other, the difference in intensities between the two sightlines helps to determine the location of the hot emitting gas. The result of our observations demonstrates that there is much less O VI emission from the Shadowed sightline than from the Unshadowed sightline. Several assumptions are made to interpret the results of our data, and under any assumptions made, the emission from inside the Local Bubble contributes only a small part of the observed emission. Thus, most of the emission originates beyond our Local Bubble. In addition, O VI emission from galactic halo would be attenuated. Therefore, most of the observed emission is related to the Loop I Superbubble itself. Further observations are required to clarify the situation.

ACKNOWLEDGEMENTS

This work was performed in collaboration with Dr. Eric Korpela, Space Sciences Laboratory, University of California at Berkeley, Berkeley, CA. We also thank W.V.D. Dixon for help with the FUSE pipeline. The author is pleased to acknowledge the UW-La Crosse College of Science and Allied Health for its financial support.

REFERENCES

Berkhuijsen, E. M., Haslam, C. G. T., & Salter, C. J. 1917, A&A, 252, 14
Cox, D. P. & Smith, B. W. 1974, ApJ, 189, L105
Dickey, J. M. & Lockman, F. J. 1990, ARA&A, 28, 215
Dixon, W. V. D., Sallmen, S., Hurwitz, M., & Lieu, R. 2001, ApJ, 552, L69
Egger, R. J. & Aschenbach, B. 1995, A&A, 294, L25
Fruscione, A., Hawkins, I., Jelinsky, P., & Wiercigroach, A. 1994, ApJS, 94, 127
Mckee, C. F. & Ostriker, J. P. 1977, ApJ, 218, 148
Moos, H. W., et al. 2000, ApJ, 538, L1
Nishikida, K. 1999, Ph.D. Thesis
Sahnow, D. J., et al. 2000, ApJ, 538, L7
Shapiro, P. R. & Field, G. B. 1976, ApJ, 205, 762
Shelton, R. L. 2002, ApJ, 569, 758
Shelton, R. L. 2003, ApJ, 589, 262
Shelton, R. L., et al. 2001, ApJ, 560, 730
Slavin, J. D. & Cox, D. P. 1993, ApJ, 417, 187
Snowden, S. L., et al. 1997, ApJ, 485, 125
Welsh, B. Y., Sallmen, S., Sfeir, D., Shelton, R. L. & Lallement, R. 2002, A&A, 394, 691